

Large Cages of Zeolitic Imidazolate Frameworks

Haoze Wang,[†] Xiaokun Pei,[†] Markus J. Kalmutzki, Jingjing Yang, and Omar M. Yaghi*



Cite This: *Acc. Chem. Res.* 2022, 55, 707–721



Read Online

ACCESS |



Metrics & More



Article Recommendations



Supporting Information

CONSPECTUS: The design and synthesis of permanently porous materials with extended cage structures is a long-standing challenge in chemistry. In this Account, we highlight the unique role of zeolitic imidazolate frameworks (ZIFs), a class of framework materials built from tetrahedral nodes connected through imidazolate linkers, in meeting this challenge and illustrate specific features that set ZIFs apart from other porous materials. The structures of ZIFs are characteristic of a variety of large, zeolite-like cages that are covalently connected with neighboring cages and fused in three-dimensional space. In contrast to molecular cages, the fusion of cages results in extraordinary architectural and chemical stability for the passage of gases and molecules through cages and for carrying out chemical reactions within these cages while keeping the cages intact. The combination of the advantages from both cage chemistry and extended structures allows uniquely interconnected yet compartmentalized void spaces inside ZIF solids, rendering their wide range of applications in catalysis, gas storage, and gas separation.

While the field of ZIFs has seen rapid development over the past decade, with hundreds of ZIF structures built from dozens of different cages of varying composition, size, and shapes reported, rational approaches to their design are largely unknown. In this Account, we summarize a vast number of cages formed in reported ZIFs and then review how the thermodynamic factors and traditional guest-templating strategies from zeolites influence the formation of cages. We highlight how the link–link interactions perform in the ZIF formation mechanism and serve as a means to target the formation of frameworks containing cages of specific sizes with structures exhibiting a level of complexity as yet unachieved in discrete coordination cages. For example, the giant *ucb* cage features a dimension of 46 Å and the complex *moz* cage is constructed from as many as 660 components.

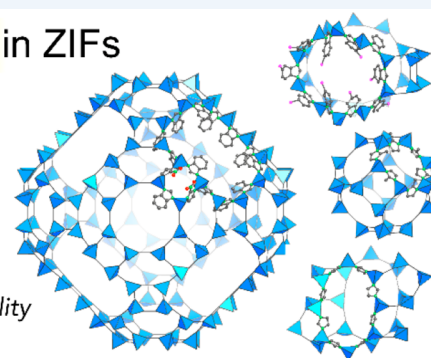
With the finding of these large and complex cages in ZIFs, we envision that the collection of cage structures will further be diversified by a mixed-linker approach utilizing a more complex combination of link–link interactions or by creating multivariant (MTV) systems that have been realized in other framework materials yet not widely employed in ZIFs. The more complicated cage structures can provide extra variations in chemical environments, and in addition to that, MTV systems can generate inhomogeneity inside each type of cage structure. The fused cages at such complexity that are difficult to be realized in solution environments will potentially enable more complex materials for smart applications.

Cages in ZIFs

Rigidity

Diversity

Designability



KEY REFERENCES

- Yang, J.; Zhang, Y.-B.; Liu, Q.; Trickett, C. A.; Gutiérrez-Puebla, E.; Monge, M. A.; Cong, H.; Aldossary, A.; Deng, H.; Yaghi, O. M. Principles of Designing Extra-Large Pore Openings and Cages in Zeolitic Imidazolate Frameworks. *J. Am. Chem. Soc.* **2017**, 139, 6448–6455.¹ *The work describes a general approach toward synthesizing large cages in ZIFs using a combination of linkers with different steric features. The discovery of the new design principle led to the largest cage that has ever been reported in ZIFs.*
- Wang, B.; Côté, A. P.; Furukawa, H.; O’Keeffe, M.; Yaghi, O. M. Colossal Cages in Zeolitic Imidazolate Frameworks as Selective Carbon Dioxide Reservoirs. *Nature* **2008**, 453, 207–211.² *The paper reports one of the early attempts to synthesize large cages in ZIFs. The cage moz was obtained in ZIF-100, with it being the most complex ZIF cage discovered so far with 264 nodes and 396 edges.*
- Banerjee, R.; Phan, A.; Wang, B.; Knobler, C.; Furukawa, H.; O’Keeffe, M.; Yaghi, O. M. High-Throughput Synthesis of Zeolitic Imidazolate Frameworks and Application to CO₂ Capture. *Science* **2008**, 319, 939–943.³ *The work provides an overview of the ZIFs structures and cages, demonstrating great potential in the structural diversity of ZIF cages.*
- Hayashi, H.; Côté, A. P.; Furukawa, H.; O’Keeffe, M.; Yaghi, O. M. Zeolite A Imidazolate Frameworks. *Nat. Mater.* **2007**, 6, 501–506.⁴ *The concept of “link–link*

Received: November 29, 2021

Published: February 16, 2022



interaction” was first discussed in this article for the synthetic design of ZIFs.

1. INTRODUCTION

Our fascination with cage compounds stems from their beauty and the promise that the space encompassed by these cages can be used to manipulate and transform confined molecules in ways not possible otherwise.⁵ Fundamental to this vision is the ability to create cages that are (a) architecturally stable to withstand the passage of gases and molecules in and out of such cages, and (b) thermally and chemically stable to allow chemistry to be carried out within these cages as well as on these cages themselves. In the 1970s, the idea that weak noncovalent interactions can be used to direct the assembly of large structures yielded the first cage-like compounds.^{6,7} Their unique properties with respect to molecular recognition processes sparked the interest in further exploring the chemistry of this class of materials. Thus far, a myriad of metal–organic coordination cages, formed through the assembly of typical neutral organic linker molecules (e.g., pyridyl-based linkers) and single metal nodes, has been reported.^{8–13} However, they generally suffer from inherent architectural instability. This makes it impossible to remove guest molecules from within these cages without collapsing them, thus limiting their applications.¹⁴

When charged linkers, such as carboxylates, are used to join the metal ions into cages, multimetallic units known as secondary building units (SBUs) become the vertices leading to the formation of metal–organic polyhedra (MOPs).¹⁵ Although a less known fact, it is these MOPs that were proven to have combined architectural, thermal, and chemical stability. We note that architectural stability is evidenced by the measurement of nitrogen adsorption isotherms at 77 K and low pressure, which was demonstrated to be possible on MOP-50 for the first time in cage-like structures.¹⁶ Although the solution host–guest chemistry of coordination cages is well-known, neither their gas adsorption isotherms nor their thermal and chemical stability has been directly evaluated prior to MOP-50.

All molecular porous entities, regardless of their chemical composition, suffer a significant inherent drawback. Although the cages themselves have defined connectivity, their spatial arrangements are impacted more by solvation status in solution states or interactions with guest molecules in solid states. This leads to the perspective of comparing coordination cages with a class of unique cage structures, zeolitic imidazolate frameworks (ZIFs). ZIFs are porous framework materials that feature a wide range of large, zeolite-like cages formed by linking single metal ion vertices and ditopic imidazole-based linkers.^{17–20} The cages in ZIFs are fused in three-dimensional space, resulting in extraordinary architectural and chemical stability that surpasses other cage-like structures. The thus-obtained well-defined spatial arrangement and alignment of cages in extended structures enabled the vast potential of ZIFs in applications related to catalysis, gas storage, and gas separation, among others.^{21–25} These ultimate extended cage compounds, in comparison to isostructural zeolites, have shown more diversified and ultralarge pore structures, resulting in a rich yet relatively unexplored field of reticular chemistry. As such, it is essential to evaluate existing ZIF structures from cage chemistry perspective for the rational design of new cage structures.

In light of the emergence of ZIFs, it is worthwhile to examine discrete coordination cage chemistry and compare it to that of

ZIFs. In this Account, we focus on the chemistry of coordination cages and ZIFs. Both classes of materials possess cage structures that are made up of single metal vertices with bridging linkers. The fundamental difference between the two is that in coordination cages the individual cages are isolated, whereas in ZIFs the cages are covalently coupled to neighboring cages. Furthermore, coordination cages are usually made of neutral pyridyl linkers, while ZIFs are made of charged imidazolate linkers. We will discuss how the structural chemistry of ZIFs fundamentally endows them with structural diversity and tunability, and outstanding architectural, chemical, and thermal stability. We also note that, as methods for making nanosized ZIF crystals become available and more developed, it is unclear, aside from the point of view of aesthetics and pure scientific inquiry, how the chemistry of coordination cages might diverge from that of *polycages* present in ZIFs.

2. ORIGINS OF THE STABILITY OF EXTENDED TETRAHEDRAL STRUCTURES

Architectural stability is a prerequisite for permanent porosity. Its origin is found in two structural features of reticular compounds: the rigidity of the individual building units and an arrangement of links around individual nodes that results in zero stress at the node itself. Framework structures built from rigid organic linkers and polynuclear SBUs often combine the rigidity of the individual building units and structural arrangements that allow all external forces to be canceled out at the nodes.²⁶ This is not possible for structures built from single metal nodes because the coordination geometry of these nodes is not as rigid as that of the SBUs in MOFs; for instance, the displacement of the metal ions perpendicular to the plane of two-dimensional coordination geometries (e.g., trigonal, square) is easy. Consequently, coordination cages generally suffer from low architectural stability (Figure 1A). The architectural instability originating from the single metal nodes can be circumvented by fusing individual cages into three-dimensional framework structures. Links connecting individual cages can be envisioned as braces that counter external forces acting on the cage upon mechanical stress. As a result, all forces exerted on the framework cancel out at the 4-c tetrahedral node (points of “zero stress”) (Figure 1B). The permanent porosity of zeolites is due to these structural features (tetrahedral nodes connected by short linkers), and the structural similarity with ZIF suggests that their stability is of the same origin.

Aside from architectural stability, chemical stability is another critical factor when considering the application of porous materials. Many studies have shown that ZIF possesses outstanding chemical stability.²⁷ This is ascribed to the fact that charged imidazolate linkers form strong bonds with metal ions. Compared with the neutral ligands utilized in constructing discrete coordination cages, charged linkers in ZIFs increase the strengths of N-metal bonds and balance the charge of cationic metal ions, allowing the formation of a stable charge neutral framework while retaining high porosity without counterions filling the pores. In addition, the imidazolate linkers lead to hydrophobic and chemically inert pore surfaces. It makes the polar species hardly attack the N-metal bonds, mitigating linker replacement and framework degradation.²⁰ These considerations are supported by the finding that ZIFs retain both crystallinity and porosity when refluxed in water, alkaline solutions, or organic solvents over an extended time.²⁷

ZIFs are well-known for their high thermal stability compared to other inorganic–organic hybrid materials. They generally

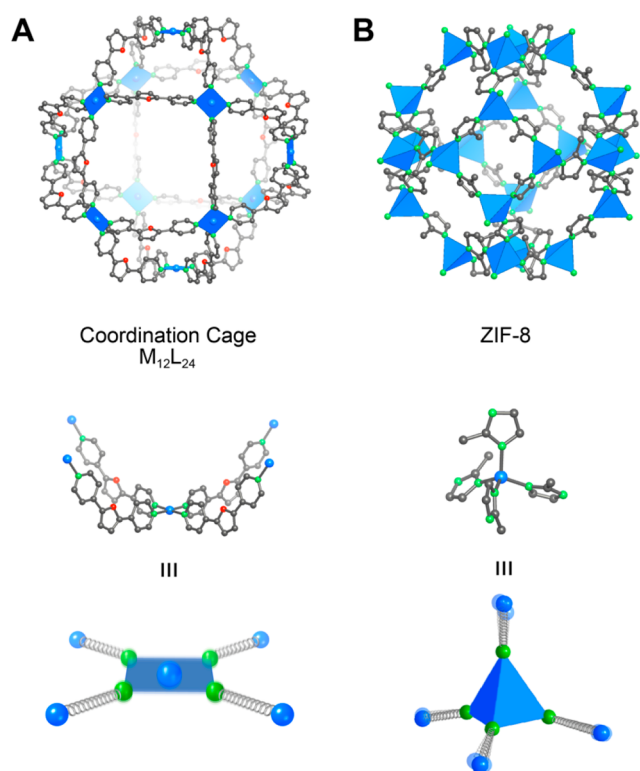


Figure 1. Comparison of the architectural stability of the planar nodes of coordination cages and tetrahedral nodes of ZIFs. (A) The planar coordination leaves one degree of freedom perpendicular to the plane for the complex, thus rendering the resulting construct architecturally unstable. (B) In extended structures built from tetrahedral nodes, this degree of freedom is removed and the displacement of the metal center is strongly aggravated. Mechanical stress acting on these nodes is more evenly distributed, rendering materials with tetrahedral topologies as architecturally stable. The use of the short imidazolate linkers in ZIFs results in additional stiffening of the overall structure. Color code: Zn, Pd, blue (tetrahedron, square or sphere); O, red; N, green; C, dark gray. Hydrogen atoms are omitted for clarity.

remain stable until around 500 °C in thermal gravimetric analyses (TGA), while MOFs usually start to decompose at around 300 °C because of decarboxylation reactions. Interestingly, a TGA-mass spectrometry (MS) analysis of ZIF-8 reported that the thermal transformation of ZIF-8 started at 400 °C was originated from the leaving of CH₃ groups, while the imidazole rings bridging metals remained to be intact and the skeleton of the framework was preserved.²⁸ The complete decomposition of the ZIF-8 framework occurs after 600 °C, during which the imidazole rings are disintegrated.²⁹

Because porous ZIFs are metastable phases, they can transform into denser and thermodynamically more stable phases when exposed to external stimuli such as pressure or temperature. A number of ZIFs can undergo glassification when glass transition temperatures are lower than the decomposition temperature.^{30,31} Mechanistic studies indicated that the coordination distortion of tetrahedral metal ions and ultrafast ligand exchange drove the amorphization at the melting stage, such that the metals in solidified glass retained their tetrahedral coordination geometry.^{32,33} Nevertheless, the ZIFs are not considered to be decomposed but collapsed in such cases.

The effects of temperature and pressure on the solvothermal and mechanochemical synthesis of ZIFs are also evident. For instance, the reaction of Co(NO₃)₂·6H₂O and 2-nitroimidazole

(nIM) in DEF at 120 °C for 12 h yields the kinetic product with a **rho** net. Prolonged heating leads to a structural transformation into a thermodynamically more stable product with a **sod** net.³⁴ Mechanical energy can also induce phase transitions as illustrated by the mechanochemical synthesis of ZIF: a low-density structure is often formed first and then evolves into increasingly dense structures in a stepwise mechanism resembling Ostwald's rule of stage.^{35,36}

ZIFs have demonstrated certain degrees of stability that are desirable to render them suitable for catalysis, gas storage, and gas separation processes. In a manner akin to other functional materials, the properties of ZIFs are strongly correlated to the structure and chemical nature of their building units. Thus, designing their structures rationally is critical in developing high-performance materials.

3. DESIGN OF ZIFs THROUGH LINK-LINK INTERACTIONS

The reticular syntheses of metal-organic frameworks rely mainly on the use of secondary building units with predefined geometries, and their principles based on geometric consideration, such as the concept of minimal transitivity, have been proposed.^{37,38} In contrast, ZIFs are solely built from imidazolate linkers and tetrahedral metals nodes, meaning that the framework structures must be determined by other interactions. Such interaction may result from the building units and the solvents used, structure-directing agents, and structural fragments formed throughout the synthesis.

Consequently, early synthetic explorations of ZIFs relied heavily on a trial-and-error approach and the use of high-throughput methods.^{3,27} This resulted in the rather serendipitous discovery of ZIF structures (Figure 5; Scheme S1) such as ZIF-10 (**mer** net) with *mer* cages [Zn₃₂(IM)₄₈, where IM = imidazolate], ZIF-8 (**sod** net) with *sod* cages [Zn₂₄(mIM)₃₆, where mIM = 2-methylimidazolate], or ZIF-11 (**rho** net) and ZIF-20 (**lta** net), whose structures both contain *lta* cages [Zn₄₈(bIM)₇₂ and Zn₄₈(Pur)₇₂, where bIM = benzimidazolate and Pur = purinate].^{3,4,27,39} The use of progressively larger imidazole-based linkers such as 5,6-dimethylbenzimidazole (HdmbIM) and 5-chlorobenzimidazole (HcbIM) was found to lead to the formation of ZIFs with larger cages: **zea** TIF-1 with *zea* cages [Zn₆₄(dmbIM)₉₆], **poz** ZIF-95 with *poz* A [Zn₄₈(cbIM)₇₂], *poz* B [Zn₈₀(cbIM)₁₂₀], and *poz* C [Zn₂₄(cbIM)₃₂] cages, and **moz** ZIF-100 with *moz* cages [Zn₂₆₄(cbIM)₃₉₆].^{2,40} While appending short side chains onto the backbones of organic linkers in MOFs has little influence on their reticulation [e.g., the isoreticular functionalization of MOF-5],⁴¹ the above examples highlight the sensitivity of ZIF formation to the steric demand and chemical nature of additional substituents appended to the imidazolate linkers.

The observed profound impact of linker substitution patterns on the net of the resulting framework is attributed to link-link interactions, including hydrogen bonding, dipole-dipole interaction, $\pi \cdots \pi$ attractions, and steric repulsion.⁴ In contrast to MOFs, where the general applicability of the isoreticular principle in expanding a given structure has been proved, such expansions are rarely possible in ZIFs. This is attributed to the fact that the angle between adjacent nodes needs to remain roughly 145° in zeolite and ZIF topologies, however, it is challenging to design isoreticular expansion of imidazolate linkers matching the required angle. How these interactions direct the formation of ZIFs becomes evident when investigating structural intermediates. Framework formation is initiated by

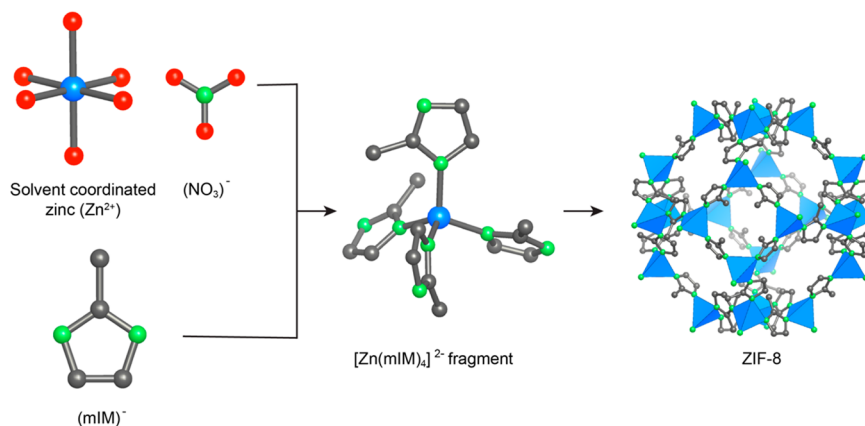


Figure 2. Formation mechanism of ZIFs exemplified by ZIF-8. Tetrahedral $\text{Zn}(\text{mIM})_4$ units are initially formed in high concentrations and persist throughout the formation of crystalline product, highlighting the influence of link–link interactions in the reticulation process. Color code: Zn, blue (tetrahedron or sphere); O, red; N, green; C, dark gray. Hydrogen atoms are omitted for clarity.

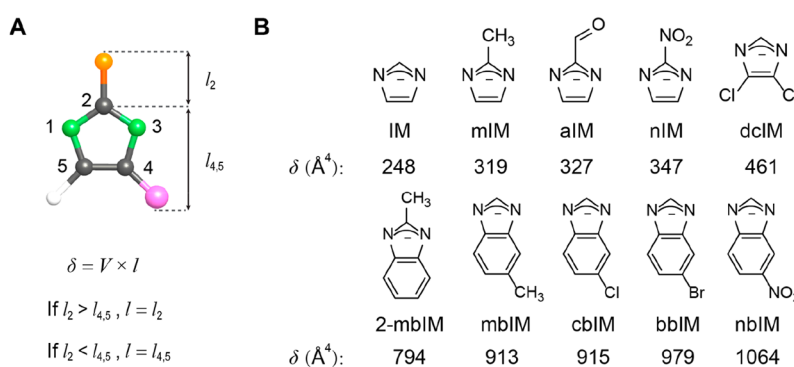


Figure 3. Link–link interactions as a design tool for ZIFs. (A) Definition of the steric index (δ). Two distances, l_2 and $l_{4,5}$, are defined, of which only the larger value is used for the calculation of the steric index. (B) Compilation of imidazole and benzimidazole derivative alongside the respective δ values. Color code: N, green; C, gray; substituents in the 2-, 4-, and 5-positions are shown in yellow, pink, and white, respectively.

the deprotonation of the imidazole linker to yield an ionic N-donor that binds to a metal ion. Synchrotron X-ray atomic pair distribution function (PDF) analysis combined with mass spectrometry, electron microscopy, and density functional theory (DFT) calculations carried out on ZIF-8 $[\text{Zn}(\text{mIM})_2]$, where $\text{mIM} = 2\text{-methylimidazolate}$ revealed that initially high concentrations of $\text{Zn}(\text{mIM})_4$ units are formed that persist over a long time (Figure 2).⁴² The formation of these moieties increases the acidity of the remaining N–H bonds, thus speeding up their deprotonation. As a result, an amorphous phase was formed that shows structural resemblance to the structure of ZIF-8 and possibly acts as an intermediate to crystalline ZIF-8. In basic solution, ZIFs typically precipitate almost instantaneously as highly insoluble powders, making it necessary to slow down the reaction by liquid diffusion, solvothermal methods, or the addition of coordination buffers in order to yield crystalline materials.

A general growth mechanism of ZIFs is thus deduced. It is initiated by the formation of small entities (i.e., clusters) by a coagulation reaction. These clusters coalesce by adding monomers to form amorphous particles, a monomer-addition that subsequently transforms into the crystalline structure by particle reorganization induced by intraparticle nucleation. The initial formation of $\text{M}(\text{IM})_4$ clusters highlights the effect that the substituent appended to the imidazole linker can exert on the way these units will link up and eventually transform into the final framework structure. Interactions between adjacent linkers

can either be attractive or repulsive, leading to either the formation of smaller or larger rings, respectively. An example for the occurrence of attractive forces between neighboring linkers is the formation of *lta* frameworks over *dia*, *sod*, and *rho* frameworks using purinate, 5-azabenzimidazolate (5-abIM), 4-azabenzimidazolate (4-abIM), and benzimidazolate (bIM) linkers (Scheme S1).²⁷ While repulsive forces are dominant for bIM and 4-abIM, the C–N bonds of both Pur and 5-abIM linkers can undergo attractive dipole–dipole interactions. As a result, these linkers assemble into small four-membered rings that subsequently form the cubic *lta* cages necessary for the construction of *lta* frameworks. In the case of bIM and 4-abIM linkers, repulsive forces direct the self-assembly process, leading to the preferential formation of large rings and thus *sod* or *rho*, and *dia* frameworks, respectively (Figure 5). While the influence of attractive dipole–dipole interactions is hard to predict, the degree of steric repulsion between differently sized imidazolate-based linkers can be quantified using the steric index δ .¹ δ is calculated according to eq 1 by multiplying the van der Waals volume of the linker molecule (V) and a distance (l) that is defined by the largest substituent. Since imidazole can be functionalized in two distinct positions, the 2-position and the 4- or 5-position, the two distance l_2 and $l_{4,5}$ have been defined (Figure 3A).

$$\delta = Vl \quad (1)$$

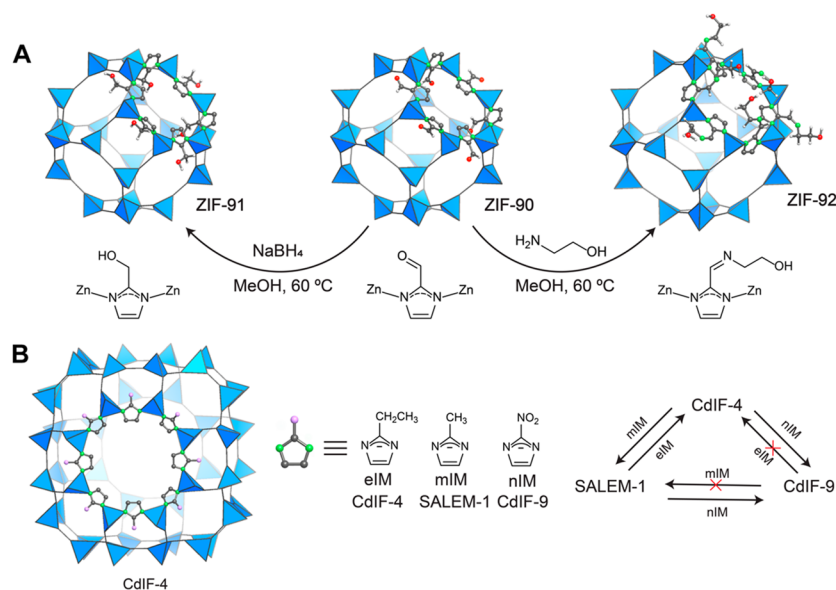


Figure 4. Postsynthetic modification of ZIFs. (A) Covalent organic modification of the organic backbone of ZIF-90. The aldehyde functionality of the aIM linker can react with an amine to give the corresponding imine (right) or reduced to give the corresponding alcohol (left). (B) Linker exchange reactions in CdIF-4. The eIM linker in CdIF-4 can be exchanged to give CdIF-9 and SALEM-1. Color code: Zn, Cd, blue (tetrahedron); O, red; N, green; C, dark gray; H, light gray; substituents in the 2-position of linkers are shown in light purple.

The steric index δ can be used to predict the size of the cages and pore openings of ZIF structures and explains the structural diversity accessible through the mixed-linker approach. Selected examples of imidazolate-based linkers alongside values of their steric indices are given in Figure 3B. The steric index of linkers used in the construction of ZIFs can give information about the size of rings formed, and thus to some degree, the size of cages constructed from these rings. This is possible based on systematic patterns found for the orientation of differently substituted imidazole-based linkers with respect to the rings formed by linking these molecules: (i) Substituents appended to the 2-position of the imidazole linker generally point into the small (mostly 4-membered) rings. (ii) Substituents appended to the 4- and 5-position of the imidazole linker are typically oriented toward the center of 8-membered and larger rings. (iii) Both substituents appended to the 2- or 4-/5-positions of the imidazole linker can point into 6-membered rings. More general principles can be derived using these findings. Increasing the size of substituents in the 4-/5-position will inevitably lead to the formation of large rings, but the simultaneous formation of smaller rings is not precluded since the sterically less demanding 2-position can point toward the center of the small rings.

Similarly, the use of imidazole-based linkers with large δ due to a large value of $l_{4,5}$ does not necessarily result in large cages because the formation of large cages (or large internal pores) in tetrahedral structures relies on a combination of both large and small rings. Accordingly, ZIF structures containing large cages are realized when both linkers with small and large δ are mixed in an appropriate ratio. This statement can be illustrated by comparing the largest cages in the structures of ZIF-68 [Zn(bIM)(nIM), where nIM = 2-nitroimidazolate] and ZIF-412 [Zn(bIM)_{1.13}(nIM)_{0.62}(IM)_{0.25}].^{1,3} While both structures contain the same 8- and 12-membered rings as a result of the high steric index of the bIM ($\delta = 679 \text{ \AA}^4$) and nIM ($\delta = 347 \text{ \AA}^4$) linkers, the *gme* cage in ZIF-68 is only half the size of the *ucb* cage in ZIF-412. This finding can be attributed to the larger number

of small rings formed by the additional comparatively small IM linkers ($\delta = 248 \text{ \AA}^4$) (Figure 3B and Figure 5).

Interestingly, multinary mixtures do not necessarily yield only one structure, but different mixtures with varying ratios of the same linkers result in the formation of frameworks with ring and pore sizes of any value up to a maximum value. The larger the number of different imidazole-based linkers incorporated into a single framework structure, the more potent this principle gets, highlighting that the number of structures accessible by linking tetrahedra is close to infinite. This statement is underpinned by the finding that reaction of Zn²⁺ ions with mixtures of nbIM ($\delta = 1064 \text{ \AA}^4$), mIM ($\delta = 319 \text{ \AA}^4$), and IM linkers ($\delta = 248 \text{ \AA}^4$) in different ratios yields three topologically distinct ZIFs; ZIF-486 [Zn(nbIM)_{0.20}(mIM)_{0.65}(IM)_{1.15}, *gme*], ZIF-376 [Zn(nbIM)_{0.25}(mIM)_{0.25}(IM)_{1.5}, *lta*], and ZIF-414 [Zn(nbIM)_{0.91}(mIM)_{0.62}(IM)_{0.47}, *ucb*] with cages-sizes being 22.6, 27.5, and 45.8 Å, respectively (Figure 5).¹

Because link–link interactions are relatively weak, the reaction medium [i.e., solvents or other structure directing agents (SDA)] may very well play a pivotal role in directing the reticulation of ZIFs, however, it is difficult to quantify these effects. Employing SDAs such as bulky amides solvents can lead to the formation of multiple structures from the very same mixture of building units. For instance, the reaction of Zn²⁺ and HIM leads to the formation of a ZIF in *can* net (CAN-[Zn₁₈(IM)₂₁]) when *N,N*-dibutylformamide (DBF) is used, but a ZIF in *afi* net (AFI-[Zn₂₄(IM)₃₀]) forms in the presence of *N,N*-dipropylformamide (DPF).⁴³ The single-crystal structure of *can* ZIF revealed that the DBF molecules reside orderly in the *can* channel, indicating that they serve as a template during ZIF formation.

More recent efficient syntheses of ZIF by liquid-assisted grinding (LAG) and ion- and liquid-assisted grinding (ILAG) were reported as well as other nontraditional synthesis routes such as sonochemical and dry-gel conversion (DGL).^{36,44} Gas sorption experiments indicate the formation of highly porous materials with specific surface areas similar to those of materials

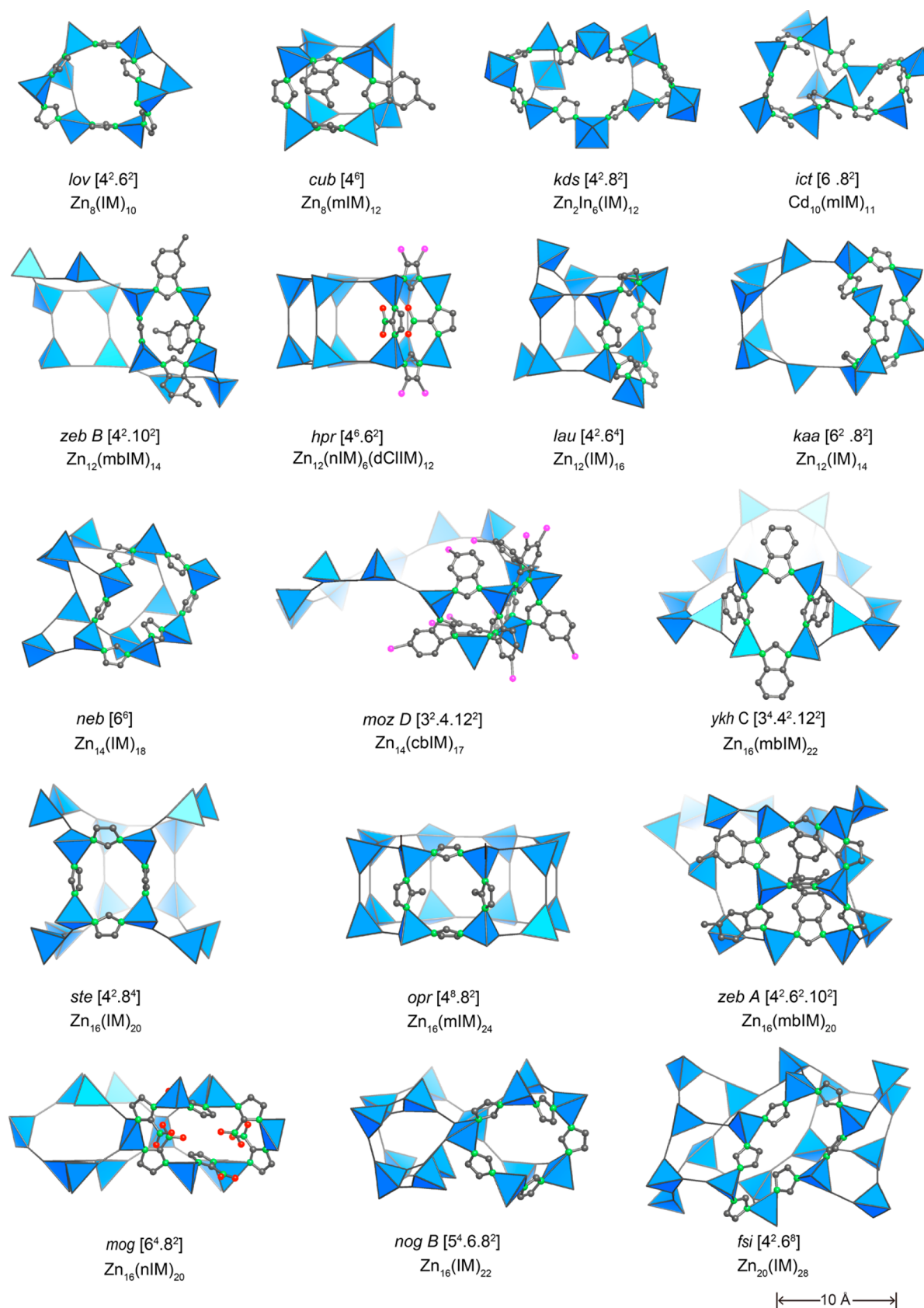


Figure 5. continued

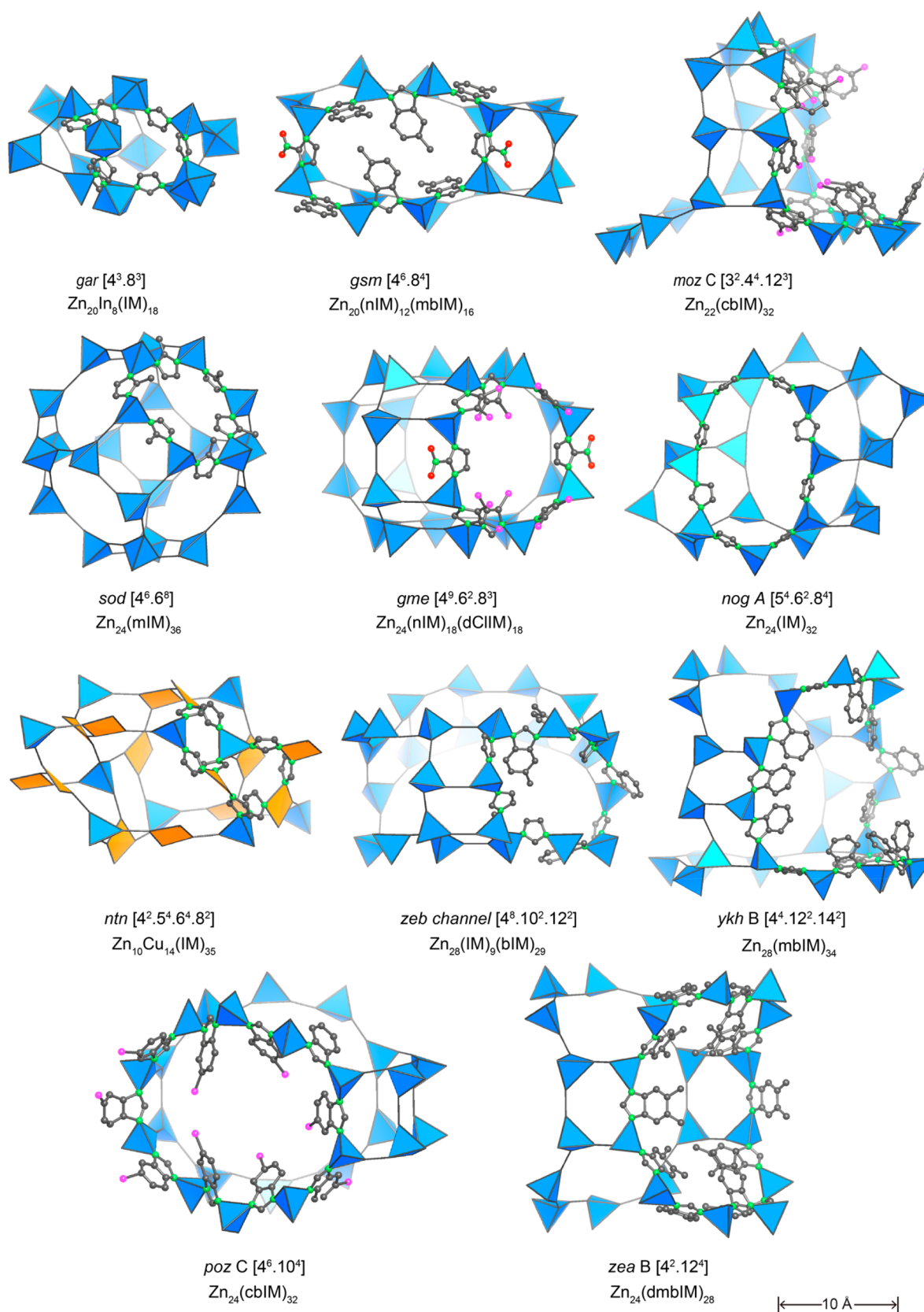


Figure 5. continued

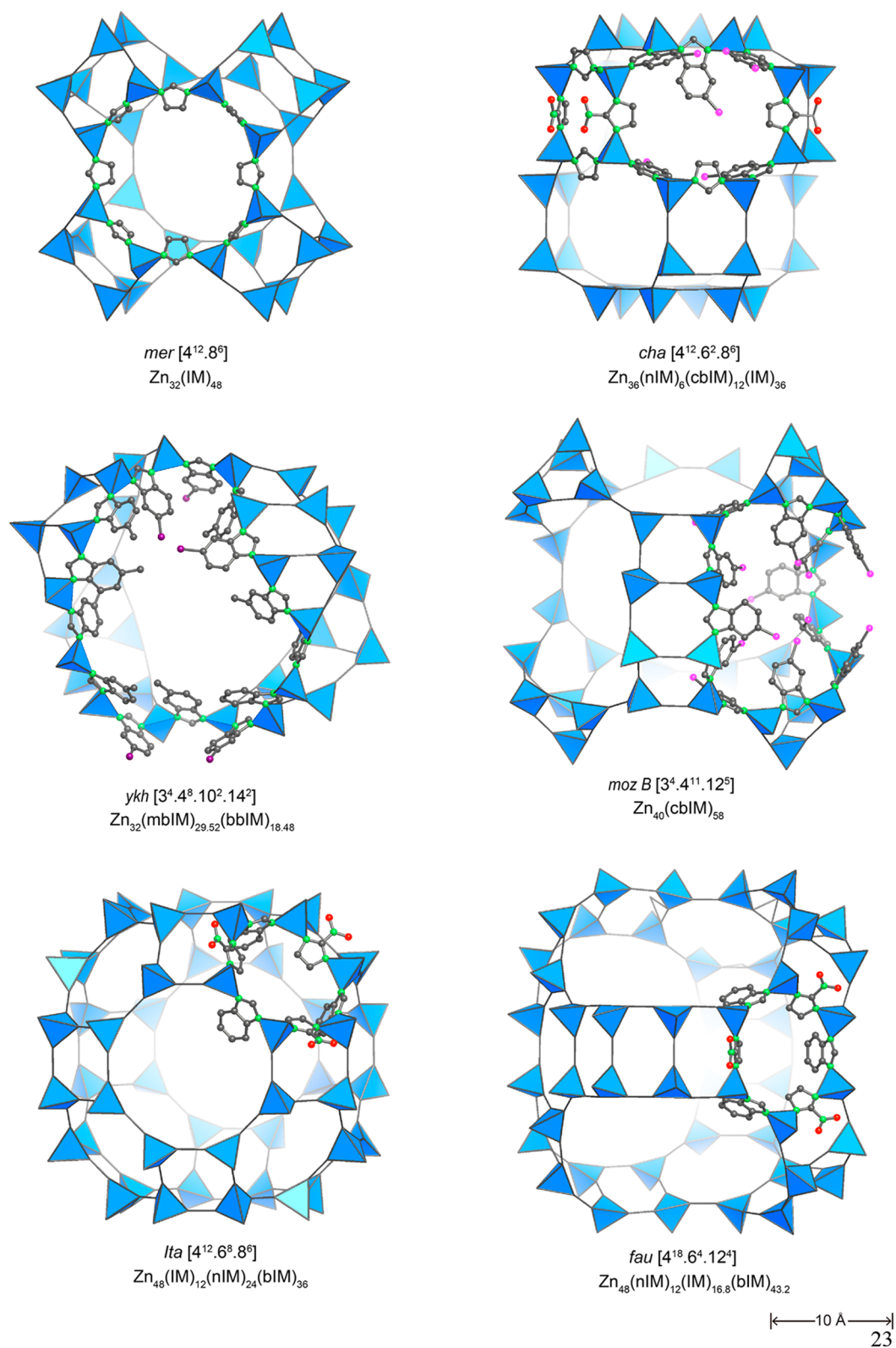


Figure 5. continued

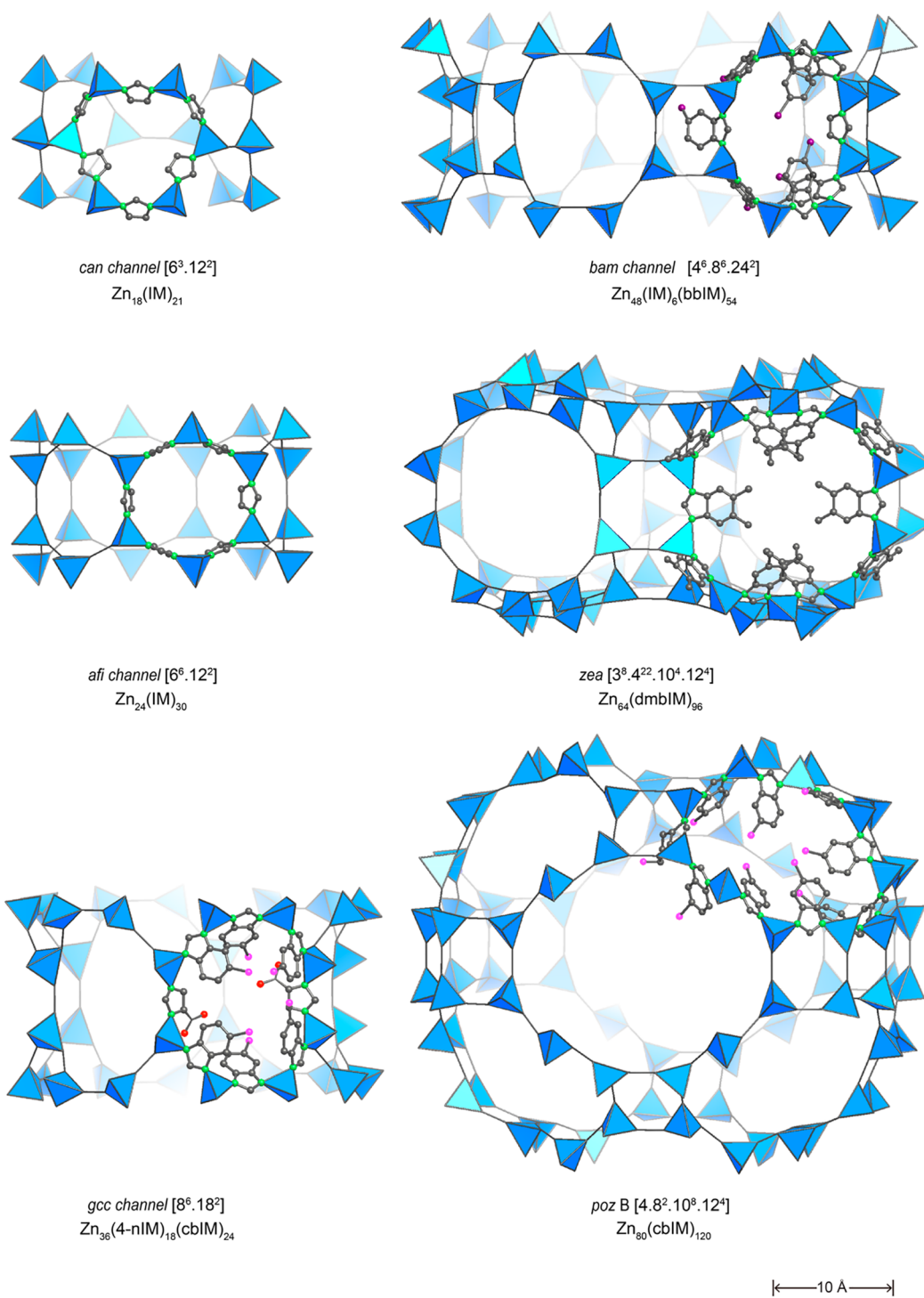


Figure 5. continued

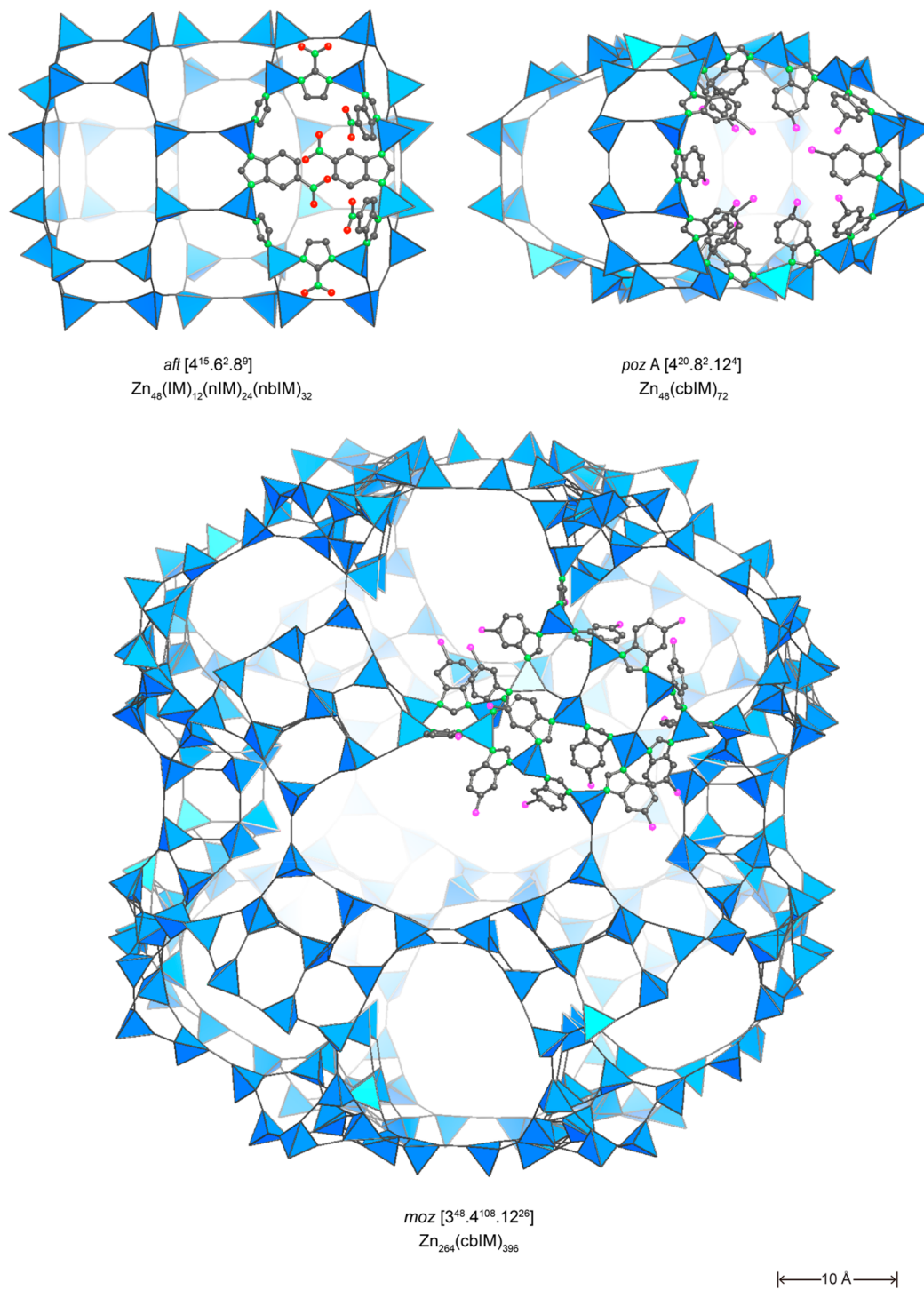


Figure 5. continued

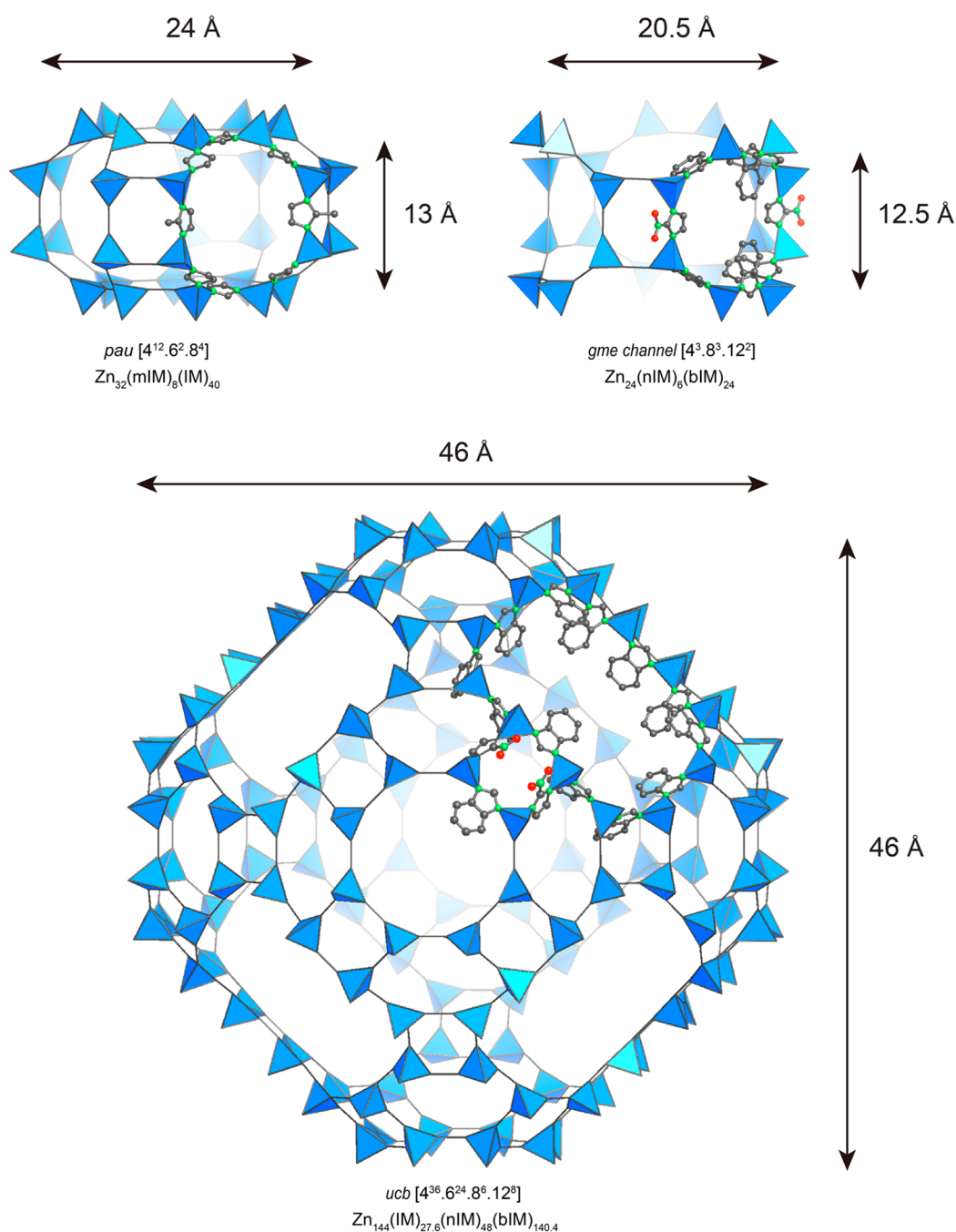


Figure 5. Cages identified in ZIFs. Color code: Zn, blue (tetrahedron); Cu, orange (square); O, red; N, green; C, dark gray; Cl, pink, Br, purple. Hydrogen atoms are omitted for clarity.

prepared by traditional solvothermal reactions. In contrast to other methods, mechanochemistry provides a tool to study the phase diagram of ZIFs, giving access to both kinetic, highly porous phases and thermodynamically more stable, dense phases. In addition, mechanochemistry allows the synthesis of ZIF phases not accessible using solvothermal methods.³⁵ In line with solvothermal synthesis, the mechanochemical reaction of ZnO and HmIM leads to the formation of ZIF-8 (**sod** net), which shows amorphization upon prolonged LAG. Further grinding results in the formation of a ZIF with **kat** net, not accessible under solvothermal conditions, and eventually a ZIF of **dia** net. These transformations follow the order of increasing

T/V ratio (2.4, 3.8, and 4.2 nm⁻³, respectively) and thus increasing thermodynamic stability.

While design principles based on a deeper understanding of the link–link interactions are useful in designing new ZIFs, they also outline the limits of direct synthesis of functionalized ZIFs. In contrast to MOFs, where isoreticular functionalization is generally applicable, for ZIFs, a specific structure can only be formed from certain combinations of metal ions and linkers, thus often precluding the formation of functionalized isoreticular derivatives via direct synthesis. This, however, does not limit the structural chemistry of ZIFs since the organic nature of the imidazole-based linkers enables their modification via postsynthetic methods.⁴⁵ An early example of a postsynthetic

modification (PSM) carried out on the organic backbone of a ZIF is the functionalization of the aIM (1*H*-imidazole-2-carbaldehyde) linkers in ZIF-90 [Zn(aIM)₂] by imine condensation with ethanolamine to yield ZIF-92, and its selective reduction using NaBH₄ to yield an alcohol group (ZIF-91).⁴⁶ In both cases, the crystallinity and porosity of the parent ZIF-90 are fully retained (Figure 4A). As an alternative to their covalent modification, the imidazole-based linkers in ZIFs can be exchanged postsynthetically (Figure 4B). These aspects further enrich the structural diversity of ZIFs.

4. DIVERSITY OF ZIF STRUCTURES AND CAGES

While only 255 zeolite structures have been reported after more than 150 years of research in this field,⁴⁷ since the first report of ZIFs in the early 2000s, ZIFs adopting more than 40 different topologies have been reported.^{1,19,20} Although composed of similar building units, ZIFs adopt many more topologies not known in zeolite chemistry. One of the reasons is that ZIFs allow multiple kinds of linkers to coexist in the same structure. This allows for one additional parameter to be tuned, a parameter not accessible for discrete coordination cages that do not allow for this degree of structural complexity. In the following section, the structural diversity of ZIFs will be discussed with respect to composition, topologies, and pore metrics.

The report of the binary mixed-linker ZIFs demonstrates the potential of the multilinker approach (see Table S1). Selecting different combinations of linkers leads to the formation of different types of rings that assemble into cages. For example, while mIM linkers, when reacted with Zn²⁺ ions, tend to form only *sod* cages and thus frameworks of *sod* net, mixing these linkers with 5-cbIM leads to the formation of both *sod* and *ucb* cages, resulting in the construction of an *lta* structure (ZIF-76) (Figure 5).

The mixed linker approach has recently been pushed to the next level by employing up to three different imidazole-based linkers simultaneously, leading to the discovery of 15 ZIFs (ZIF-303, 360, 365, 376, 386, 408, 410, 412, 413, 414, 486, 516, 586, 615, and 725).¹ This strategy facilitates the formation of ZIFs with 10 different nets, among them previously unreported nets such as *kfi*, *afx*, *ucb*, *ykh*, *gcc*, and *bam*, from a selection of only ten different linkers. Such structural complexity can only be achieved by mixing multiple linkers within one structure and has seldom been observed in any other cage compounds or cage-containing materials. The mixed linker approach does, however, not preclude the formation of simple structures previously realized in binary systems, such as ZIF-303 [Zn-(cbIM)_{0.70}(nIM)_{0.30}(IM)_{1.00}, *cha* net], ZIF-376 [Zn-(nbIM)_{0.25}(mIM)_{0.25}(IM)_{1.50}, *lta* net], ZIF-410 [Zn-(cbIM)_{1.10}(aIM)_{0.90} *gme* net], and ZIF-486 [Zn-(nbIM)_{0.20}(mIM)_{0.65}(IM)_{1.15}, *gme* net].

The vast number of accessible structures entails the prospect of precisely tailored pore metrics (cage size and aperture size) and shapes. These features are of key importance not only for the preparation of highly porous materials for gas storage applications but also for selective trapping of molecules in separation processes, catalysis, and drug capture/release processes to name a few. The cages in ZIF structures are commonly referred to with their net acronym as given in the RCSR database (lower case three-letter code, italicized), or, more intuitively, their face symbols. The face symbol [...n^m...] provides information on the types and connections of rings giving the number (m) of n-membered rings (MRs) found on the surface of the cage.⁴⁸ In contrast to molecular cages that are

most often built from only small rings (e.g., 3-, 4-, 5-, and 6-MRs), the library of accessible rings is much larger in ZIFs, where 8-, 10-, 12-, 14-, 18-, and even 24-MRs are frequently encountered. The combination of many rings of different sizes is the key to constructing giant cages such as the *ucb* cage in ZIF-412 having the face symbol [4³⁶.6²⁴.8⁶.12⁸]. Each *ucb* cage is composed of 36 4-MRs, 24 6-MRs, 6 8-MRs, and 8 12-MRs. The *ucb* cage represents the largest cages ever achieved in porous tetrahedral crystals; one single *ucb* cage can store as many as 121 octane or 146 *p*-xylene molecules at 298 K. A list of reported ZIF compositions along with information on their nets and the cages their structures are built from can be found in Table S1.

With respect to selective capture or release processes, not only the size but also the precise shape of the pores are of pivotal importance. Forty-six different porous cages with various shapes and pore openings have been identified in ZIFs (Figure 5). Depending on their shape, these cages can be classified as (i) nearly spherical, (ii) ellipsoidal, (iii) irregular, and (iv) channels. Cages of regular spherical shape are referred to as “nearly spherical cages” and include *sod*, *cha*, *lta*, *fau*, *moz*, and *ucb* cages. The high point symmetry of these cages typically imparts a high symmetry onto the framework itself. For instance, the *fau* and *ucb* cages found in *ucb* ZIF-412 (*Fm* $\bar{3}$ *m*) have point symmetries of 43*m* and *m* $\bar{3}$ *m*, respectively, and the *lta* cages found in LTA (*Pm* $\bar{3}$ *m*), RHO (*Pm* $\bar{3}$ *m*), KFI (*Im* $\bar{3}$ *m*), and *ucb* (*Fm* $\bar{3}$ *m*) ZIFs and have a point symmetry of *m* $\bar{3}$ *m*. The highly symmetric cages in ZIFs are almost “isotropic”, and their indistinguishable subcomponents/faces help to minimize the surface energy and distribute local strain equally throughout the assembly.⁴⁹ In combination with the fact that each vertex of these cages is linked to another cage, this results in the outstanding architectural stability of ZIFs. As a result, the cage sizes and the complexity of their architecture exceed those of the most sophisticated discrete molecular cage compound ever made (Pd₄₈L₉₆ with 48 Pd nodes and 96 linkers)¹³ by far: A single cage built from up to 264 nodes that are connected by 396 linkers as in the case of the *moz* cage.² The immense structural diversity found in the realm of ZIFs known today is most likely only the tip of the iceberg, and it can be expected that the further development of the multilinker approach will give rise to a myriad of new ZIF structures.

5. INTRINSIC ADVANTAGES OF FUSED CAGES

Extended structures built from fused cages present the following advantages: the chemical and architectural stability from the interconnected vertices, and the fact of being able to connect a variety of cages with different chemical environments in closely confined spaces in a well-defined spatial arrangement. These two features, together with the large surface area and tunable pore size, provide ZIFs with unique potentials among cage-like materials with respect to their future development and application.

The benefit of the excellent stability of ZIFs has been demonstrated in several applications, such as being effective heterogeneous catalysts for several reactions. For example, ZIF-8, ZIF-9, and ZIF-10 exhibited outstanding performance in catalyzing the Knoevenagel reaction between benzaldehyde and malononitrile, without showing structural degradation in the basic reaction media.⁵⁰ Hupp et al. exchanged the mIM linker of ZIF-8 into imidazolate (IM) followed by the treatment with *n*-butyl lithium,⁵¹ targeting at the formation of a solid-state Brønsted base catalyst. It is not only a clear example of the chemical stability of ZIF-8 toward strong nucleophilic bases, but

also of the architectural stability of being able to bear linker exchange without degrading into other topologies.

Multivariate systems, i.e., structures built from a combination of multiple interchangeable linkers bearing identical binding groups but being chemically distinct, promise even greater potential.⁵² It was shown that the performance of MTV-MOFs often surpasses that of corresponding individual non-MTV-MOFs due to synergy effects.⁵³ A mixed-linker ZIF-8 composed of 2-methylimidazole (HmIM) and 1,2,4-triazole (Hmtz) can be viewed as the simplest model of a MTV-ZIF.⁵⁴ The two kinds of linkers were found to be randomly distributed throughout the crystals, and varying the linker ratios allowed the fine-tuning of the threshold pressure of capillary condensation of their water sorption isotherms. Although MTV-ZIFs with more than two kinds of linkers have not been reported, it is anticipated that a higher complexity and better performances will be achieved when increasing the type of linkers in MTV-ZIFs.

Fusing cages into extended structures allows several different cages to coexist in the same crystal, creating a complex platform joining distinct chemical environments in an ordered spatial arrangement. In contrast to discrete cage systems, the different cages in ZIFs are connected in a face sharing manner, allowing the guest molecules to travel through the cages on a predefined path given by the spatial arrangement of the cages with respect to each other, which is not possible for individual molecular cages. Additionally, the imidazolate linkers can guide molecules through the pore system by directing them via steric effects. A study on ZIF-8 revealed that the mass transport within the cages occurs $\sim 10^2$ times (at 200 K) more than that between cages, while the gate opening effect allows for the cross-cage migration to be tuned at higher pressures and temperatures.⁵⁵

Looking at ZIFs as individual but fused cages, they can be viewed as compartmentalized not only in terms of space and geometry, but also in terms of function. Their cages have varying chemical compositions and geometries and thus possess different properties such as polarities, resulting in different behavior in physical processes. For example, the in situ X-ray diffraction experiment on ZIF-412 found that its cages were sequentially filled during the gas sorption process: first the *lta* cage, then the *fau* cage, and eventually the largest *ucb* cage.⁵⁶ This concept can be applied to the design of materials where each individual cage has a specific function as can be envisioned for ZIF-reactors: cascade reactions are carried out in the individual cages and the substrate is guided from one cage-reactor to another until the final product is formed. Such materials provide chemists with the opportunity to carry out complex multistep reaction within a single material. This prospect is unique to ZIFs because they are the only group of compounds featuring a fixed spatial arrangement of cages that are interconnected through small apertures, which is not possible for MOFs or arrangements of MOPs as both MOFs and MOPs feature pores without wall, rather than cages.

Fast guest molecule diffusion is indeed the basis of the application of ZIFs in gas storage and separation. Arranging various linkers in ZIFs provide the opportunity to fabricate remarkably large and complex cages, which benefit the removal of large volatile organic compounds (e.g., octane and *p*-xylene) in particular,¹ and facilitate the diffusion of guests across the crystal. Engineering approaches can further help to improve the mass transport in ZIFs by making ZIFs into nanosized particles,⁵⁷ thin films,⁵⁸ or permeable nanostructures.⁵⁹ Combining the hierarchical pore structure and material

fabrication techniques will allow us to optimize the performances of this solid-state porous material to the greatest extent.

6. OUTLOOK

ZIFs are a unique class of materials that combine the advantages of cages and architecturally stable extended structures. Over the last decades, dozens of cages with various compositions, sizes, and shapes have been discovered, exhibiting a level of complexity that cannot be realized in molecular cages. Their unique architecture and high mechanical, chemical, and thermal stability combined with the possibility of postsynthetic modification renders them a highly promising class of materials for a wide range of applications including but not limited to gas storage, gas separation, and catalysis. The potential of ZIFs with respect to structural complexity has, however, not been realized to its full extent.⁶⁰ While the link–link interactions play a pivotal role in understanding ZIF formation, further research is required to fully understand the mechanism of ZIF formation and thus deduce principles allowing for the design and synthesis of ZIFs with ever growing complexity. This will eventually allow for the in silico design of high performance ZIFs and a profound understanding of structure–property relationships even for highly complex multinary structures. The combination of traits of different classes of materials with those of ZIFs will further enrich the realm of ZIF chemistry, as was recently shown for Z-MOFs, materials implementing elements of ZIF and MOF chemistry. Therefore, the progress made in ZIF chemistry over the course of the past decade represents only a glimpse of their vast largely unexplored potential.

■ ASSOCIATED CONTENT

Supporting Information

The Supporting Information is available free of charge at <https://pubs.acs.org/doi/10.1021/acs.accounts.1c00740>.

Common linkers in ZIFs and the abbreviation of their names, nets can be formed by varying the combination of linkers of ZIFs, cages that are only found in ZIFs, zeolite cages that are found in ZIFs (PDF)

■ AUTHOR INFORMATION

Corresponding Author

Omar M. Yaghi – Department of Chemistry, University of California–Berkeley, Berkeley, California 94720, United States; Kavli Energy NanoScience Institute at UC Berkeley, Berkeley, California 94720, United States; Joint UAEU-UC Berkeley Laboratories for Materials Innovations, UAE University, Al Ain, United Arab Emirates; orcid.org/0000-0002-5611-3325; Email: yaghi@berkeley.edu

Authors

Haoze Wang – Department of Chemistry, University of California–Berkeley, Berkeley, California 94720, United States; Kavli Energy NanoScience Institute at UC Berkeley, Berkeley, California 94720, United States

Xiaokun Pei – Department of Chemistry, University of California–Berkeley, Berkeley, California 94720, United States; Kavli Energy NanoScience Institute at UC Berkeley, Berkeley, California 94720, United States; orcid.org/0000-0002-6074-1463

Markus J. Kalmutzki – Department of Chemistry, University of California–Berkeley, Berkeley, California 94720, United

States; Kavli Energy NanoScience Institute at UC Berkeley, Berkeley, California 94720, United States

Jingjing Yang – Department of Chemistry, University of California–Berkeley, Berkeley, California 94720, United States; Kavli Energy NanoScience Institute at UC Berkeley, Berkeley, California 94720, United States; orcid.org/0000-0002-1192-7368

Complete contact information is available at:

<https://pubs.acs.org/10.1021/acs.accounts.1c00740>

Author Contributions

[†]H.W. and X.P. contributed equally. The manuscript was written with contributions from all authors. All authors have approved the final version of the manuscript.

Funding

The authors appreciate the support of UAE University under the UAEU-UC Berkeley Laboratories for Materials Innovations.

Notes

The authors declare no competing financial interest.

Biographies

Haoze Wang is currently a Ph.D. candidate at the University of California, Berkeley in the group of Prof. Omar M. Yaghi. After completing his bachelor's degree at Zhejiang University, he moved to Berkeley to pursue his doctorate in Chemistry. His research is focused on the design and synthesis of new reticular materials.

Xiaokun Pei is currently a Ph.D. candidate in chemistry at the University of California, Berkeley. Xiaokun received her Bachelor of Science from Beijing Institute of Technology in 2016. Her research interest in Prof. Omar M. Yaghi's lab focuses on the characterizations of reticular materials using single-crystal X-ray diffraction.

Markus J. Kalmutzki was a *Deutsche Forschungsgemeinschaft* postdoctoral fellow in Prof. Omar M. Yaghi's lab from 2015 to 2018. Markus earned his diploma in Chemistry from the University of Tuebingen in 2010, where he also received his Ph.D. in 2014. He worked with Prof. H.-Juergen Meyer as a postdoctoral fellow from 2014 to 2015. He is currently a research and development engineer at Baxter International Inc.

Jingjing Yang was a graduate student in Prof. Omar M. Yaghi's lab at the University of California, Berkeley. He received his Ph.D. degree in Chemistry in 2018. After working with Prof. Colin Nuckolls at Columbia University for his postdoctoral research, he is now a research scientist at the General Electric Company.

Omar M. Yaghi is currently the James and Neeltje Tretter Professor of Chemistry, University of California, Berkeley, and a senior faculty scientist at Lawrence Berkeley National Laboratory. His research encompasses stitching together organic and inorganic molecules by strong bonds to make crystalline extended porous structures, such as metal–organic frameworks, zeolitic imidazolate frameworks, and covalent organic frameworks. He named this field reticular chemistry.

REFERENCES

- (1) Yang, J.; Zhang, Y.-B.; Liu, Q.; Trickett, C. A.; Gutiérrez-Puebla, E.; Monge, M. A.; Cong, H.; Aldossary, A.; Deng, H.; Yaghi, O. M. Principles of Designing Extra-Large Pore Openings and Cages in Zeolitic Imidazolate Frameworks. *J. Am. Chem. Soc.* **2017**, *139*, 6448–6455.
- (2) Wang, B.; Côté, A. P.; Furukawa, H.; O'Keeffe, M.; Yaghi, O. M. Colossal Cages in Zeolitic Imidazolate Frameworks as Selective Carbon Dioxide Reservoirs. *Nature* **2008**, *453*, 207–211.
- (3) Banerjee, R.; Phan, A.; Wang, B.; Knobler, C.; Furukawa, H.; O'Keeffe, M.; Yaghi, O. M. High-Throughput Synthesis of Zeolitic Imidazolate Frameworks and Application to CO₂ Capture. *Science* **2008**, *319*, 939–943.
- (4) Hayashi, H.; Côté, A. P.; Furukawa, H.; O'Keeffe, M.; Yaghi, O. M. Zeolite A Imidazolate Frameworks. *Nat. Mater.* **2007**, *6*, 501–506.
- (5) Chakrabarty, R.; Mukherjee, P. S.; Stang, P. J. Supramolecular Coordination: Self-Assembly of Finite Two- and Three-Dimensional Ensembles. *Chem. Rev.* **2011**, *111*, 6810–6918.
- (6) Pedersen, C. J. Cyclic Polyethers and Their Complexes with Metal Salts. *J. Am. Chem. Soc.* **1967**, *89*, 7017–7036.
- (7) Dietrich, B.; Lehn, J. M.; Sauvage, J. P.; Blanzat, J. Cryptates—X Syntheses et Propriétés Physiques de Systèmes Diaza-Polyoxa-Macrocycliques. *Tetrahedron* **1973**, *29*, 1629–1645.
- (8) Fujita, M.; Oguro, D.; Miyazawa, M.; Oka, H.; Yamaguchi, K.; Ogura, K. Self-Assembly of Ten Molecules into Nanometre-Sized Organic Host Frameworks. *Nature* **1995**, *378*, 469–471.
- (9) Fujita, M.; Ogura, K. Supramolecular Self-Assembly of Macrocycles, Catenanes, and Cages through Coordination of Pyridine-Based Ligands to Transition Metals. *Bull. Chem. Soc. Jpn.* **1996**, *69*, 1471–1482.
- (10) Takeda, N.; Umamoto, K.; Yamaguchi, K.; Fujita, M. A Nanometre-Sized Hexahedral Coordination Capsule Assembled from 24 Components. *Nature* **1999**, *398*, 794–796.
- (11) Tominaga, M.; Suzuki, K.; Kawano, M.; Kusakawa, T.; Ozeki, T.; Sakamoto, S.; Yamaguchi, K.; Fujita, M. Finite, Spherical Coordination Networks That Self-Organize from 36 Small Components. *Angew. Chem., Int. Ed.* **2004**, *43*, 5621–5625.
- (12) Sun, Q.-F.; Iwasa, J.; Ogawa, D.; Ishido, Y.; Sato, S.; Ozeki, T.; Sei, Y.; Yamaguchi, K.; Fujita, M. Self-Assembled M₂₄L₄₈ Polyhedra and Their Sharp Structural Switch upon Subtle Ligand Variation. *Science* **2010**, *328*, 1144–1147.
- (13) Fujita, D.; Ueda, Y.; Sato, S.; Mizuno, N.; Kumasaka, T.; Fujita, M. Self-Assembly of Tetravalent Goldberg Polyhedra from 144 Small Components. *Nature* **2016**, *540*, 563–566.
- (14) Ueda, Y.; Ito, H.; Fujita, D.; Fujita, M. Permeable Self-Assembled Molecular Containers for Catalyst Isolation Enabling Two-Step Cascade Reactions. *J. Am. Chem. Soc.* **2017**, *139*, 6090–6093.
- (15) Tranchemontagne, D. J.; Ni, Z.; O'Keeffe, M.; Yaghi, O. M. Reticular Chemistry of Metal–Organic Polyhedra. *Angew. Chem., Int. Ed.* **2008**, *47*, 5136–5147.
- (16) Sudik, A. C.; Millward, A. R.; Ockwig, N. W.; Côté, A. P.; Kim, J.; Yaghi, O. M. Design, Synthesis, Structure, and Gas (N₂, Ar, CO₂, CH₄, and H₂) Sorption Properties of Porous Metal–Organic Tetrahedral and Heterocuboidal Polyhedra. *J. Am. Chem. Soc.* **2005**, *127*, 7110–7118.
- (17) Chen, B.; Yang, Z.; Zhu, Y.; Xia, Y. Zeolitic Imidazolate Framework Materials: Recent Progress in Synthesis and Applications. *J. Mater. Chem. A* **2014**, *2*, 16811–16831.
- (18) Tan, J. C.; Bennett, T. D.; Cheetham, A. K. Chemical Structure, Network Topology, and Porosity Effects on the Mechanical Properties of Zeolitic Imidazolate Frameworks. *Proc. Natl. Acad. Sci. U. S. A.* **2010**, *107*, 9938–9943.
- (19) Phan, A.; Doonan, C. J.; Uribe-Romo, F. J.; Knobler, C. B.; O'Keeffe, M.; Yaghi, O. M. Synthesis, Structure, and Carbon Dioxide Capture Properties of Zeolitic Imidazolate Frameworks. *Acc. Chem. Res.* **2010**, *43*, 58–67.
- (20) Zhang, J.-P.; Zhang, Y.-B.; Lin, J.-B.; Chen, X.-M. Metal Azolate Frameworks: From Crystal Engineering to Functional Materials. *Chem. Rev.* **2012**, *112*, 1001–1033.
- (21) Aceituno Melgar, V. M.; Kim, J.; Othman, M. R. Zeolitic Imidazolate Framework Membranes for Gas Separation: A Review of Synthesis Methods and Gas Separation Performance. *J. Ind. Eng. Chem.* **2015**, *28*, 1–15.
- (22) Lai, L. S.; Yeong, Y. F.; Keong Lau, K.; Azmi, M. S. Zeolitic Imidazolate Frameworks (ZIF): A Potential Membrane for CO₂/CH₄ Separation. *Sep. Sci. Technol.* **2014**, *49*, 1490–1508.
- (23) Barkholtz, H. M.; Liu, D.-J. Advancements in Rationally Designed PGM-Free Fuel Cell Catalysts Derived from Metal–Organic Frameworks. *Mater. Horizons* **2017**, *4*, 20–37.

- (24) Mottillo, C.; Friščić, T. Carbon Dioxide Sensitivity of Zeolitic Imidazolate Frameworks. *Angew. Chem., Int. Ed.* **2014**, *53*, 7471–7474.
- (25) Pimentel, B. R.; Parulkar, A.; Zhou, E.; Brunelli, N. A.; Lively, R. P. Zeolitic Imidazolate Frameworks: Next-Generation Materials for Energy-Efficient Gas Separations. *ChemSusChem* **2014**, *7*, 3202–3240.
- (26) Yaghi, O. M.; O’Keeffe, M.; Ockwig, N. W.; Chae, H. K.; Eddaoudi, M.; Kim, J. Reticular Synthesis and the Design of New Materials. *Nature* **2003**, *423*, 705–714.
- (27) Park, K. S.; Ni, Z.; Côté, A. P.; Choi, J. Y.; Huang, R.; Uribe-Romo, F. J.; Chae, H. K.; O’Keeffe, M.; Yaghi, O. M. Exceptional Chemical and Thermal Stability of Zeolitic Imidazolate Frameworks. *Proc. Natl. Acad. Sci. U. S. A.* **2006**, *103*, 10186–10191.
- (28) Gadipelli, S.; Travis, W.; Zhou, W.; Guo, Z. A Thermally Derived and Optimized Structure from ZIF-8 with Giant Enhancement in CO₂ Uptake. *Energy Environ. Sci.* **2014**, *7*, 2232–2238.
- (29) Gadipelli, S.; Guo, Z. X. Tuning of ZIF-Derived Carbon with High Activity, Nitrogen Functionality, and Yield – A Case for Superior CO₂ Capture. *ChemSusChem* **2015**, *8*, 2123–2132.
- (30) Bennett, T. D.; Goodwin, A. L.; Dove, M. T.; Keen, D. A.; Tucker, M. G.; Barney, E. R.; Soper, A. K.; Bithell, E. G.; Tan, J.-C.; Cheetham, A. K. Structure and Properties of an Amorphous Metal–Organic Framework. *Phys. Rev. Lett.* **2010**, *104*, 115503.
- (31) Bennett, T. D.; Cheetham, A. K. Amorphous Metal–Organic Frameworks. *Acc. Chem. Res.* **2014**, *47*, 1555–1562.
- (32) Gaillac, R.; Pullumbi, P.; Beyer, K. A.; Chapman, K. W.; Keen, D. A.; Bennett, T. D.; Coudert, F.-X. Liquid Metal–Organic Frameworks. *Nat. Mater.* **2017**, *16*, 1149–1154.
- (33) Bennett, T. D.; Tan, J.-C.; Yue, Y.; Baxter, E.; Ducati, C.; Terrill, N. J.; Yeung, H. H.-M.; Zhou, Z.; Chen, W.; Henke, S.; Cheetham, A. K.; Greaves, G. N. Hybrid Glasses from Strong and Fragile Metal–Organic Framework Liquids. *Nat. Commun.* **2015**, *6*, 8079.
- (34) Biswal, B. P.; Panda, T.; Banerjee, R. Solution Mediated Phase Transformation (RHO to SOD) in Porous Co-Imidazolate Based Zeolitic Frameworks with High Water Stability. *Chem. Commun.* **2012**, *48*, 11868–11870.
- (35) Katsenis, A. D.; Puškarić, A.; Štrukil, V.; Mottillo, C.; Julien, P. A.; Užarević, K.; Pham, M.-H.; Do, T.-O.; Kimber, S. A. J.; Lazić, P.; Magdysyuk, O.; Dinnebier, R. E.; Halasz, I.; Friščić, T. In Situ X-Ray Diffraction Monitoring of a Mechanochemical Reaction Reveals a Unique Topology Metal–Organic Framework. *Nat. Commun.* **2015**, *6*, 6662.
- (36) Do, J.-L.; Friščić, T. Mechanochemistry: A Force of Synthesis. *ACS Cent. Sci.* **2017**, *3*, 13–19.
- (37) Yaghi, O. M.; O’Keeffe, M.; Ockwig, N. W.; Chae, H. K.; Eddaoudi, M.; Kim, J. Reticular Synthesis and the Design of New Materials. *Nature* **2003**, *423*, 705–714.
- (38) Kalmutzki, M. J.; Hanikel, N.; Yaghi, O. M. Secondary Building Units as the Turning Point in the Development of the Reticular Chemistry of MOFs. *Sci. Adv.* **2018**, *4*, No. eaat9180.
- (39) Huang, X.; Zhang, J.; Chen, X. [Zn(Bim)₂] · (H₂O)_{1.67}: A Metal–Organic Open-Framework with Sodalite Topology. *Chin. Sci. Bull.* **2003**, *48*, 1531–1534.
- (40) Wu, T.; Bu, X.; Liu, R.; Lin, Z.; Zhang, J.; Feng, P. A New Zeolitic Topology with Sixteen-Membered Ring and Multidimensional Large Pore Channels. *Chem. - Eur. J.* **2008**, *14*, 7771–7773.
- (41) Eddaoudi, M.; Kim, J.; Rosi, N.; Vodak, D.; Wachter, J.; O’Keeffe, M.; Yaghi, O. M. Systematic Design of Pore Size and Functionality in Isorecticular MOFs and Their Application in Methane Storage. *Science* **2002**, *295*, 469–472.
- (42) Terban, M. W.; Banerjee, D.; Ghose, S.; Medasani, B.; Shukla, A.; Legg, B. A.; Zhou, Y.; Zhu, Z.; Sushko, M. L.; De Yoreo, J. J.; Liu, J.; Thallapally, P. K.; Billinge, S. J. L. Early Stage Structural Development of Prototypical Zeolitic Imidazolate Framework (ZIF) in Solution. *Nanoscale* **2018**, *10*, 4291–4300.
- (43) Shi, Q.; Xu, W.-J.; Huang, R.-K.; Zhang, W.-X.; Li, Y.; Wang, P.; Shi, F.-N.; Li, L.; Li, J.; Dong, J. Zeolite CAN and AFI-Type Zeolitic Imidazolate Frameworks with Large 12-Membered Ring Pore Openings Synthesized Using Bulky Amides as Structure-Directing Agents. *J. Am. Chem. Soc.* **2016**, *138*, 16232–16235.
- (44) Lee, Y.-R.; Jang, M.-S.; Cho, H.-Y.; Kwon, H.-J.; Kim, S.; Ahn, W.-S. ZIF-8: A Comparison of Synthesis Methods. *Chem. Eng. J.* **2015**, *271*, 276–280.
- (45) Wang, Z.; Cohen, S. M. Postsynthetic Modification of Metal–Organic Frameworks. *Chem. Soc. Rev.* **2009**, *38*, 1315–1329.
- (46) Morris, W.; Doonan, C. J.; Furukawa, H.; Banerjee, R.; Yaghi, O. M. Crystals as Molecules: Postsynthesis Covalent Functionalization of Zeolitic Imidazolate Frameworks. *J. Am. Chem. Soc.* **2008**, *130*, 12626–12627.
- (47) Zeolite Framework Types. *Database of Zeolite Structures*. https://asia.iza-structure.org/IZA-SC/ftc_table.php (accessed 2021-09-27).
- (48) Blatov, V. A.; O’Keeffe, M.; Proserpio, D. M. Vertex-, Face-, Point-, Schläfli-, and Delaney-Symbols in Nets, Polyhedra and Tilings: Recommended Terminology. *CrystEngComm* **2010**, *12*, 44–48.
- (49) Beuerle, F. Unexplored Territory for Self-Assembly. *Nature* **2016**, *540*, 529–530.
- (50) Tran, U. P. N.; Le, K. K. A.; Phan, N. T. S. Expanding Applications of Metal–Organic Frameworks: Zeolite Imidazolate Framework ZIF-8 as an Efficient Heterogeneous Catalyst for the Knoevenagel Reaction. *ACS Catal.* **2011**, *1*, 120–127.
- (51) Karagiari, O.; Lalonde, M. B.; Bury, W.; Sarjeant, A. A.; Farha, O. K.; Hupp, J. T. Opening ZIF-8: A Catalytically Active Zeolitic Imidazolate Framework of Sodalite Topology with Unsubstituted Linkers. *J. Am. Chem. Soc.* **2012**, *134*, 18790–18796.
- (52) Deng, H.; Doonan, C. J.; Furukawa, H.; Ferreira, R. B.; Towne, J.; Knobler, C. B.; Wang, B.; Yaghi, O. M. Multiple Functional Groups of Varying Ratios in Metal–Organic Frameworks. *Science* **2010**, *327*, 846–850.
- (53) Dong, Z.; Sun, Y.; Chu, J.; Zhang, X.; Deng, H. Multivariate Metal–Organic Frameworks for Dialing-in the Binding and Programming the Release of Drug Molecules. *J. Am. Chem. Soc.* **2017**, *139*, 14209–14216.
- (54) Zhang, J.; Zhu, A.; Lin, R.; Qi, X.; Chen, X. Pore Surface Tailored SOD-Type Metal–Organic Zeolites. *Adv. Mater.* **2011**, *23*, 1268–1271.
- (55) Jobic, H.; Kolokolov, D. I.; Stepanov, A. G.; Koza, M. M.; Ollivier, J. Diffusion of CH₄ in ZIF-8 Studied by Quasi-Elastic Neutron Scattering. *J. Phys. Chem. C* **2015**, *119*, 16115–16120.
- (56) Cho, H. S.; Yang, J.; Gong, X.; Zhang, Y.-B.; Momma, K.; Weckhuysen, B. M.; Deng, H.; Kang, J. K.; Yaghi, O. M.; Terasaki, O. Isotherms of Individual Pores by Gas Adsorption Crystallography. *Nat. Chem.* **2019**, *11*, 562–570.
- (57) Nune, S. K.; Thallapally, P. K.; Dohnalkova, A.; Wang, C.; Liu, J.; Exarhos, G. J. Synthesis and Properties of Nano Zeolitic Imidazolate Frameworks. *Chem. Commun.* **2010**, *46*, 4878–4880.
- (58) Huang, A.; Chen, Y.; Wang, N.; Hu, Z.; Jiang, J.; Caro, J. A Highly Permeable and Selective Zeolitic Imidazolate Framework ZIF-95 Membrane for H₂/CO₂ Separation. *Chem. Commun.* **2012**, *48*, 10981–10983.
- (59) Shen, K.; Zhang, L.; Chen, X.; Liu, L.; Zhang, D.; Han, Y.; Chen, J.; Long, J.; Luque, R.; Li, Y.; Chen, B. Ordered Macro-Microporous Metal–Organic Framework Single Crystals. *Science* **2018**, *359*, 206–210.
- (60) *Atlas of Prospective Zeolite Structures*. <http://www.hypotheticalzeolites.net> (accessed 2021-09-27).